

UC Irvine

UC Irvine Previously Published Works

Title

Global Microbiota-Dependent Histone Acetylation Patterns Are Irreversible and Independent of Short Chain Fatty Acids

Permalink

<https://escholarship.org/uc/item/6cz139vj>

Journal

Hepatology, 74(6)

ISSN

0270-9139

Authors

Saiman, Yedidya
Shen, Ting-Chin David
Lund, Peder J
[et al.](#)

Publication Date

2021-12-01

DOI

10.1002/hep.32043

Peer reviewed



Published in final edited form as:

Hepatology. 2021 December ; 74(6): 3427–3440. doi:10.1002/hep.32043.

Global Microbiota-Dependent Histone Acetylation Patterns Are Irreversible and Independent of Short Chain Fatty Acids

Yedidya Saiman^{1,*}, Ting-Chin David Shen^{1,*}, Peder J. Lund², Victoria M. Gershuni³,
Cholsoo Jang^{4,*}, Shivali Patel¹,
Sunhee Jung^{*},

Emma E. Furth⁵, Elliot S. Friedman¹, Lillian Chau¹, Benjamin A. Garcia^{2,†}, Gary D. Wu¹

¹Division of Gastroenterology and Hepatology, Perelman School of Medicine, University of Pennsylvania, Philadelphia, PA

²Department of Biochemistry and Biophysics, Penn Epigenetics Institute, Perelman School of Medicine, University of Pennsylvania, Philadelphia, PA

³Department of Surgery, Perelman School of Medicine, Hospital of the University of Pennsylvania, Philadelphia, PA

⁴Department of Chemistry and Lewis-Sigler Institute for Integrative Genomics, Princeton University, Princeton, NJ

⁵Department of Pathology and Laboratory Medicine, Perelman School of Medicine, University of Pennsylvania, Philadelphia, PA

Abstract

BACKGROUND AND AIMS: Although germ-free mice are an indispensable tool in studying the gut microbiome and its effects on host physiology, they are phenotypically different than their conventional counterparts. While antibiotic-mediated microbiota depletion in conventional mice leads to physiologic alterations that often mimic the germ-free state, the degree to which the effects of microbial colonization on the host are reversible is unclear. The gut microbiota produce abundant short chain fatty acids (SCFAs), and previous studies have demonstrated a link between microbial-derived SCFAs and global hepatic histone acetylation in germ-free mice.

ADDRESS CORRESPONDENCE AND REPRINT REQUESTS TO: Gary D. Wu, M.D., Perelman School of Medicine, University of Pennsylvania, 915 BRB II/III, 421 Curie Blvd, Philadelphia, PA 19104, gdwu@pennmedicine.upenn.edu, Tel.: +1-215-898-0158.

Author Contributions: Y.S., T.D.S., P.J.L., B.A.G., and G.D.W developed the experimental ideas and design of the study. Experiments were performed by Y.S., T.D.S., P.J.L., V.M.G., C.J., S.P., S.J., E.E.F., E.S.F., and L.C. Data analysis was performed by Y.S., T.D.S., P.J.L., V.M.G., C.J., S.P., S.J., E.E.F., E.S.F., L.C. and G.D.W., Figures were produced by Y.S. and T.D.S. The text was written by Y.S., T.D.S., and G.D.W with input from all authors. G.D.W and B.A.G. supervised the study. Y.S. and T.D.S. contributed equally to this article.

*These authors contributed equally to this work.

†Current address: Department of Biological Chemistry, University of California Irvine, Irvine, CA

‡Department of Biochemistry and Molecular Biophysics, Washington University School of Medicine, St. Louis, MO

Potential conflict of interest: Dr. Friedman consults for Astarte.

Supporting Information

Additional Supporting Information may be found at onlinelibrary.wiley.com/doi/10.1002/hep.32043/suppinfo.

APPROACH AND RESULTS: We demonstrate that global hepatic histone acetylation states measured by mass spectrometry remained largely unchanged despite loss of luminal and portal vein SCFAs after antibiotic-mediated microbiota depletion. In contrast to stable hepatic histone acetylation states, we see robust hepatic transcriptomic alterations after microbiota depletion. Additionally, neither dietary supplementation with supraphysiologic levels of SCFA nor the induction of hepatocyte proliferation in the absence of microbiota-derived SCFAs led to alterations in global hepatic histone acetylation.

CONCLUSIONS: These results suggest that microbiota-dependent landscaping of the hepatic epigenome through global histone acetylation is static in nature, while the hepatic transcriptome is responsive to alterations in the gut microbiota.

Histones are a core component of eukaryotic cell chromatin structure. Histones undergo posttranslational modifications (PTMs) promoting alterations in histone–DNA interaction, transcription factor recruitment, and ultimately gene regulation.⁽¹⁾ Specifically, histone acetylation is a tightly regulated process governed by a dynamic balance between histone acetyltransferases (HATs) and histone deacetylases (HDACs). Together, regulation of these enzymes, along with the abundance of their substrate acetyl–coenzyme A (CoA), comprise a major mechanism of gene regulation.⁽²⁾

Global histone acetylation results in histone alterations across the genome as opposed to specific gene loci.⁽³⁾ First described in yeast, such changes occur over large stretches of chromatin, including coding regions and nonpromoter sequences affecting genome integrity.⁽³⁾ Gene regulation by acetylation changes at specific loci as defined by chromatin immunoprecipitation (ChIP) sequencing is well defined, but genome-wide acetylation also appears to modulate transcription independent of locus specific changes.⁽⁴⁾ Global alterations in histone acetylation is linked to intracellular pH and carbon metabolism, and global hypoacetylation is characteristic of many tumors.⁽⁵⁾ In liver disease, dysregulated expression and subsequent alterations in global histone acetylation states have been implicated in the development of HCC, while aberrant HDAC expression is associated with poor patient prognosis and survival.⁽⁶⁾ Conversely, in murine models of partial hepatectomy, there is an increase in nearly all HDAC isoforms, suggesting that global decreases in histone acetylation is necessary for efficient liver regeneration.⁽⁷⁾ We therefore focused on global hepatic histone acetylation as a model to elucidate the role of microbially produced SCFAs in hepatic function

Mechanistically, it has been proposed that the production of SCFAs by the gut microbiota regulates global hepatic histone acetylation.⁽⁸⁾ SCFA activity in the liver is particularly relevant due to first-pass metabolism of intestinally derived metabolites directly delivered to the liver through the portal circulation.^(9,10) Indeed, multiple studies have demonstrated differences in liver injury between conventional and SCFA lacking germ-free mice, potentially linking these differences to alterations in histone acetylation.^(11,12) To this end, significant differences in hepatic epigenetic programming, assessed by global histone acetylation states, have been described between germ-free and conventionally housed mice in which the patterns in the latter can be recapitulated by bacterial colonization of the former

and that SCFA production by the gut microbiota is an important effector of these alterations through the regulation of histone acetylation.⁽⁸⁾

Despite the utility of germ-free mice in probing the complex interaction between the gut microbiota and host physiology, germ-free mice are developmentally, physiologically, and metabolically unique when compared with their conventionally housed counterparts.⁽¹³⁾ Combined with the difficulty and expense involved in raising gnotobiotic mice, studies have begun to use models of antibiotic-mediated microbiota depletion to mimic the germ-free state by feeding conventionally housed mice a cocktail of antibiotics. Such interventions are also more relevant to modulation of the human microbiome. Herein we sought to determine whether antibiotic-mediated microbiota depletion would affect global hepatic histone acetylation states through SCFA-dependent mechanisms, as previously observed in germ-free mice. Despite a loss of luminal SCFAs after antibiotic treatment, we found no alterations in global hepatic histone acetylation states in both proliferating and non-proliferating hepatocytes. Nonetheless, we note robust alterations in the hepatic transcriptome after microbial depletion that are independent of global histone acetylation changes. These results suggest that microbial and dietary modifications to the gut microbiome in conventionally raised mice are not a means to modulate global hepatic histone acetylation. Furthermore, microbiota-dependent landscaping of the hepatic epigenome appears static in nature, while the hepatic transcriptome is responsive to alterations in the gut microbiota, yet independent of global histone acetylation.

Materials and Methods

ANIMAL STUDIES

Animal studies followed protocols approved by the University of Pennsylvania Institutional Animal Care and Use Committee and adhere to the standards articulated in the Animal Research: Reporting of In Vivo Experiments guidelines. All mice in this study were 8–12-week-old C57Bl/6J male mice purchased from Jackson Laboratories (Bar Harbor, ME) except where otherwise noted. Mice were maintained in a standard specific pathogen-free barrier facility and fed irradiated AIN-76 chow (Research Diets, Inc., New Brunswick, NJ), unless otherwise noted. Germ-free mice were bred and housed in isolated incubators at the University of Pennsylvania Gnotobiotic Facility. Microbiota depletion of conventional mice was accomplished by oral delivery of antibiotics in sterile drinking water (1.125 g aspartame, 0.15 g vancomycin, and 0.3 g neomycin in 300 mL) for 72 hours. During the final 12 hours the mice were fasted and maintained on a 10% pegylated interferon and antibiotics solution until time of sacrifice.⁽¹⁴⁾ For acetate feeding experiments, mice were treated with antibiotics, followed by addition of 150 mM ¹²C₂ sodium acetate (Cat# S2889; Sigma-Aldrich, St. Louis, MO) or ¹³C₂ sodium acetate (Cat# 282014; Sigma-Aldrich) to their drinking water for 72 hours before sacrifice. For inulin feeding experiments, 8–12-week-old C57Bl/6J female mice were fed an iso-caloric diet supplemented with either cellulose (4.5% by weight) or inulin (17.5% by weight) for 2 weeks. For acute liver injury, mice received a single intraperitoneal injection of 2 μL/g carbon tetrachloride (CCl₄) diluted in corn oil and sacrificed at indicated timepoints.

CELL LINES AND REAGENTS

Alpha mouse liver 12 (AML12), an immortalized murine normal hepatocyte cell line, was purchased from ATCC (Cat# CRL-2254; American Type Culture Collection (Manassas, VA) and cultured per supplier's recommendations. Huh7 were cultured at 37°C and 5% CO₂ in high glucose Dulbecco's modified Eagle's medium (Invitrogen, Waltham, MA) supplemented with 10% fetal bovine serum and penicillin/streptomycin (Invitrogen).

HDAC INHIBITION ASSAY

AML12 or HUH7 cells were seeded in 96-well plates at a density of 8×10^3 cells per well and incubated overnight. HDAC inhibition was measured with increasing concentrations of sodium butyrate (Cat# 303410; Sigma-Aldrich) with HDAC-Glo I/II Assay (Promega, Madison, WI) according to manufacturer's protocol in serum free media. A total of 50 nM trichostatin A was used as a positive HDAC inhibitor control.

DNA EXTRACTION AND 16S COPY NUMBER ANALYSIS

Genomic DNA was extracted from fresh frozen feces as previously described.⁽¹⁴⁾ Bacterial 16S ribosomal RNA gene sequences were analyzed using quantitative PCR using primers binding to the V1-V2 regions, and results normalized to input DNA.⁽¹⁴⁾

HISTONE ISOLATION AND MASS SPECTROMETRY

Flash-frozen liver tissue was homogenized in a hypotonic lysis buffer and histones extracted using 0.4N H₂SO₄, trichloroacetic acid (TCA)–precipitated and derivatized as previously described.⁽⁹⁾ Digested and derivatized peptides were then desalted with C18 stage tips before analysis by liquid chromatography–tandem mass spectrometry (LC/MS-MS). Histone peptides were separated by a nanoLC system (Easy nLC1000 or Dionex UltiMate3000; Thermo Fisher Scientific, Waltham, MA) in line with a Fusion Orbitrap or QE-HF mass spectrometer (Thermo Fisher Scientific). C18 resin (ReproSil-Pur 120 C18-AQ, 3 μm; Dr. Maisch GmbH, Baden-Wuerttemberg, Germany) packed in a fused silica capillary column (75 μm i.d. × 12 cm; Polymicro Technologies, Phoenix, AZ) served as the stationary phase. Mass spectrometry for histone acetylation was performed as previously described, with typical settings for the digital image analysis scans with a resolution of 30,000, AGC 5e5, max injection time auto, and NCE 27.⁽¹⁵⁾ The relative abundances of histone peptides with different modifications were calculated based on peak areas using EpiProfile software.

SHORT CHAIN FATTY ACID MEASUREMENTS

SCFAs were derivatized with 12 mM EDC, 15 mM 3-Nitrophenylhydrazine and pyridine (2% vol/vol) in methanol, and the reaction was stopped with quenching reagent (0.5 mM beta-mercaptoethanol in water). Serum (5 μL) or feces (1 mg) was mixed with derivatizing reagent (100 μL) and incubated for 1 hour at 4°C. Samples were subsequently centrifuged at 16,000g for 10 minutes at 4°C, and 20 μL of supernatant was mixed with 200 μL of the quenching reagent. After centrifugation at 16,000g for 10 minutes at 4°C, supernatants were collected for LC/MS-MS analysis. A quadrupole time of flight mass spectrometer (Q-TOF; Agilent, Santa Clara, CA) operating in negative ion mode was coupled with C18 chromatography through electrospray ionization and used to scan from 100 to 300 m/z at

1-Hz and 15,000 resolution. LC separation was on an Acquity UPLC BEH C18 column (2.1 × 100 mm, 1.75- μ m particle size, 130 Å pore size; Waters, Milford, MA) using a gradient of solvent A (water) and solvent B (methanol). Flow rate was 200 μ L/min. The LC gradient was 0 minutes, 10% B; 1 minute, 10% B; 5 minutes, 30% B; 7 minutes, 100% B; 11 minutes, 100% B; 11.5 minutes, 10% B; 14 minutes, 10% B. Autosampler temperature was 5°C, and injection volume was 10 μ L. Ion masses for derivatized, acetate, propionate, and butyrate were 194, 208, and 222, respectively.

RNA-SEQUENCING PROCESSING AND ANALYSIS

RNA was extracted from whole-liver tissue stored in RNALater using RNeasy Mini Kit (Qiagen, Hilden, Germany). Total RNA quantity and quality were assessed with RNA ScreenTape assay of Agilent 2200 TapeStation System (Agilent Technologies, Santa Clara, CA). Libraries were prepared using TruSeq Stranded mRNA HT Sample Prep Kit (Illumina, San Diego, CA) as per standard protocol and quantified using HS D1000 ScreenTape assay of Agilent 2200 TapeStation System (Agilent Technologies). A 100-bp single-read sequencing of multiplexed samples was performed on an Illumina HiSeq 4000 sequencer. Illumina's bcl2fastq version 2.20.0.422 software was used to convert bcl to fastq files.

Raw sequence files (fastq) for 10 samples were mapped using salmon (<https://combine-lab.github.io/salmon/>) against the mouse transcripts described in genecode (version M21, built on the mouse genome GRCm38.p6; <https://www.genecodegenes.org>). Transcript counts were summarized to the gene level using tximport (<https://bioconductor.org/packages/release/bioc/html/tximport.html>), normalized and tested for differential expression using DESeq2 (<https://bioconductor.org/packages/release/bioc/html/DESeq2.html>). Normalized count data were visualized using principal component analysis to assess intersample variation, and a single outlier was excluded from subsequent analyses. To analyze global gene-expression profiles, the number of uniquely aligning read counts to mRNA transcripts in RefSeq were extracted from the RUM output and processed using a custom script to carry out differential expression analysis using Bioconductor software's package *edgeR* to compute a *P* value and fold change for each transcript. The *P* values were corrected for multiple testing using the Benjamini & Hochberg mode of the R function *p.adjust* to compute a false discovery rate (FDR).

QUANTITATIVE REAL-TIME PCR

RNA was reverse-transcribed using the High Capacity cDNA Reverse Transcription Kit (Cat# 4368814; Applied Biosystems, Waltham, MA) to generate complementary DNA (cDNA) according to manufacturer's protocol. Generated cDNA subsequently underwent quantitative PCR with Fast SYBR Green Master Mix (Cat# 4385612; Applied Biosystems) using different primers and glyceraldehyde 3-phosphate dehydrogenase as endogenous control. Primer sequences for quantitative real-time PCR are listed in Supporting Table S3. Fold change in gene expressions between control and antibiotic-treated groups was determined based on the DDCT method.⁽¹⁶⁾

STATISTICAL ANALYSIS

Data are shown as the mean with SEM. Statistical differences among groups were determined by Student *t* test, unless otherwise noted. Differences were considered statistically significant at $P < 0.05$.

DATA AVAILABILITY STATEMENT

The RNA-sequencing data sets analyzed in the current study are available at Gene Expression Omnibus, accession GSE144266. The data supporting this study are available in the article and in the Supporting Information, and available from the authors upon reasonable request.

Results

GLOBAL HEPATIC HISTONE ACETYLATION IS NOT ALTERED BY ANTIBIOTIC-MEDIATED GUT MICROBIOME DEPLETION

Germ-free mice demonstrate decreased levels of global hepatic histone acetylation compared with conventionally housed mice, a phenotype that can be partially rescued by the oral administration of SCFAs.⁽⁸⁾ We therefore hypothesized that the inverse might also be true, namely that antibiotic-mediated microbiota depletion and subsequent SCFA depletion would lead to global hepatic histone acetylation alterations. We treated mice with 3 days of nonabsorbable antibiotics and an osmotic laxative to deplete the luminal microbiota and used mass spectrometry to assess global histone acetylation states within the liver. We confirmed effective microbiota depletion after antibiotics treatment with about an 8-log decrease in stool 16S copy number as compared with control (Fig. 1A) with the subsequent loss of microbiota-derived cecal short chain fatty acids acetate, butyrate, and propionate (Fig. 1B) as well as formate (Supporting Fig. S1A). Consistent with the decrease in cecal SCFAs, there was a 2-fold, 5-fold, and >10-fold decrease in portal vein levels of acetate, butyrate and propionate, respectively, after antibiotic treatment (Fig. 1C). The relatively modest decrease in acetate and butyrate levels in the portal vein compared with the cecum likely reflects mammalian host production and metabolism of acetate and intestinal epithelial cell metabolism of butyrate.^(17,18) Portal and peripheral blood formate levels were also decreased in antibiotic-treated mice (Supporting Fig. S1B,C). Peripheral blood levels of propionate and butyrate were much lower (~10–20 fold) than portal blood levels (Fig. 1C,D), reflecting their efficient hepatic clearance. In comparison, despite the changes seen in the portal vein, there were no significant changes in peripheral blood levels of acetate after antibiotic treatment (Fig. 1D), consistent with the hepatic regulation of acetate.⁽¹⁷⁾

We next surveyed 30 unique histone acetylation PTM states on histone H3, H3.3, and H4 acid extracted histones from whole liver tissue. We observed only one statistically significant change with a modest 1.2-fold increase in histone acetylation on H4:K8acK12ac (Fig. 1E; Supporting Table S1, column A), which was contrary to our initial hypothesis. Given these unexpected results, we repeated the experiment three additional times under similar conditions (data not shown) and saw only modest alterations (not exceeding ± 1.5 -fold) in global histone acetylation states that were not consistent between experiments.

To examine whether a longer duration of microbiota and SCFA depletion has an effect, we treated mice with antibiotics for 14 days. Still, we saw almost no change of global histone acetylation (Supporting Table S1, column B). Together, these data suggest that luminal depletion of SCFAs with antibiotics does not meaningfully alter global hepatic histone acetylation states and that the inconsistent changes seen are likely a function of biological variance within histone acetylation states.

BUTYRATE LEVELS DELIVERED FROM THE GUT MICROBIOTA TO THE LIVER ARE NOT SUFFICIENT TO INHIBIT HDAC ACTIVITY

We next examined the potential role for specific luminal-derived SCFAs in regulating hepatic histone acetylation states. We reasoned that, *in vivo*, butyrate cannot affect hepatic histone acetylation, as the concentration of butyrate in the portal vein is nearly 400-fold lower than in the cecum (Fig. 1B,C) and well below the millimolar concentration required for *in vitro* HDAC inhibition.⁽¹⁹⁾ The half-maximal inhibitory concentration (IC₅₀) of HDACs by butyrate is about 1,000 μ M in cell culture,⁽²⁰⁾ suggesting that, in pharmacodynamic terms, microbial-derived butyrate is unlikely to influence hepatic histone acetylation states through HDAC inhibition. Indeed, by measuring butyrate inhibition of HDAC-1/2 in hepatocellular cell lines AML12 (Fig. 2A) and Huh7 (Fig. 2B), we show IC₅₀ values of 903 μ M and 708 μ M, respectively. Only at butyrate concentrations of >100 μ M, at least 10 times greater than physiologic levels in the portal vein, is there any evidence of HDAC inhibition in either cell line. This indicates that at physiologically relevant concentrations observed in portal vein serum, butyrate cannot mediate hepatic histone acetylation through HDAC inhibition. We therefore determined the effect of gut microbiota-derived acetate on histone acetylation.

DIETARY SUPPLEMENTATION WITH SUPRAPHYSIOLOGIC LEVELS OF ACETATE DOES NOT ALTER GLOBAL HEPATIC HISTONE ACETYLATION

The cellular pool of acetyl-CoA arises from multiple sources including acetate.⁽²⁾ Because depletion of luminal and portal vein acetate did not alter hepatic histone acetylation, we attempted to increase acetate delivery to the liver by oral supplementation with supraphysiologic levels of acetate in the drinking water.

Mice were treated with antibiotics for 3 days to eliminate microbial acetate production and then supplemented with 150 mM sodium acetate or 150 mM sodium chloride in their drinking water for 3 days. Mice treated with antibiotics and acetate drank more water than antibiotics alone (Supporting Fig. S2) and consumed about 135 mg (1.7 millimoles) of sodium acetate daily. Antibiotic treatment decreased bacterial load by about 2 log (Fig. 3A) with significant reduction in cecal acetate levels (Fig. 3B), although direct acetate feeding did not lead to an increase in cecal (Fig. 3B) or portal vein (Fig. 3C) acetate.

After acetate feeding, we observed only a single statistically significant change and a 0.7-fold decrease in peptide H3:K14ac (Supporting Table S1, column C), arguing against a direct role of luminal-derived acetate whether increasing acetate through microbial fermentation of digestible fiber would lead to changes in hepatic histone acetylation. Mice were fed diets supplemented with either a fermentable (inulin) or non-fermentable (cellulose) fiber for 2

weeks. Stool acetate levels from inulin-fed mice were 2.5-fold greater than cellulose fed mice (Fig. 3D), although no differences were seen in portal serum acetate levels (Fig. 3E). Similar to direct acetate feeding, there was only a single significant acetylation change in H4 after inulin feeding (Supporting Table S1, column D).

To demonstrate that luminal-derived acetate incorporates into hepatic histones, we performed a ^{13}C -acetate tracing study. Mice were fed ^{13}C -acetate in their drinking water for 3 days, and ^{13}C incorporation into histone acetyl groups was measured. There was a small, yet statistically significant, incorporation of ^{13}C -acetate-derived acetyl groups in mono-acetylated (Fig. 3F) and di-acetylated (Fig. 3G) H4 histones, demonstrating that the ingested acetate was incorporated into hepatic histone acetyl groups. Together these data demonstrate that microbial-derived acetate is absorbed from the gut and incorporated into histones acetyl groups. However, increased acetate consumption or production does not modulate global histone acetylation states.

MICROBIOTA-DEPENDENT SCFAs DOES NOT ALTER GLOBAL HEPATIC HISTONE ACETYLATION AFTER ACUTE CCl_4 INJURY

Acetyl-CoA-dependent histone acetylation is a key mediator of cellular proliferation.⁽²¹⁾ Under normal physiologic conditions, hepatocyte turnover is slow, but in models of liver injury and regeneration histone acetylation is associated with hepatocyte proliferation.⁽²²⁾ We therefore used a model of acute liver injury to investigate whether changes in SCFA availability may alter global histone acetylation patterns specifically during hepatocyte regeneration and proliferation. Control and antibiotic-treated mice received a single sublethal intraperitoneal dose of CCl_4 (2 $\mu\text{L}/\text{gm}$) (Fig. 4A). Mice were sacrificed at 24 and 48 hours after injury during peak hepatocyte proliferation. 16S quantitative PCR confirmed an approximate 4–5-log decrease in bacterial load after antibiotic treatment (Fig. 4B). Despite hepatic injury as noted by elevated aspartate aminotransferase (Fig. 4C) and alanine aminotransferase (Fig. 4D) levels, and tissue necrosis (Fig. 4E), at 24 and 48 hours compared with baseline, no differences were noted between control and antibiotic-treated mice. Similarly, Ki67 expression is increased in control and antibiotic-treated mice after CCl_4 administration, indicating active cellular proliferation, with no difference seen between the groups (Fig. 4F).

Finally, we assessed histone acetylation states in antibiotic-treated and untreated mice that received CCl_4 . Acute liver injury with CCl_4 led to similar histone acetylation changes in both antibiotic-treated respective uninjured control groups at both 24 and 48 hours after injury (Fig. 4G). There was a shift from poly-acetylated species to mono-acetylated species, most notably in the H4 N-terminus (H4:K5, H4:K8, H4:K12, and H4:K16), and H3:K18/K23. However, in comparing antibiotic-treated and untreated mice that both received CCl_4 at 24 and 48 hours after injury, there was almost no histone acetylation differences (Supporting Table S1, columns E and F, respectively). Together, this demonstrates that hepatic injury leads to a global shift in histone acetylation that is primarily independent of the gut microbiota.

ANTIBIOTIC-MEDIATED MICROBIOTA DEPLETION LEADS TO CHANGES IN HEPATIC AMINO ACID METABOLISM GENE EXPRESSION

Previous studies have demonstrated significant hepatic transcriptomic changes between germ-free and conventional mice with specific changes seen in xenobiotic metabolism and p450 enzymes as well as shifts in metabolic pathways and nutrient use.^(23,24) Despite no changes in global hepatic histone acetylation, we assessed the effects of antibiotic-mediated microbiome depletion on hepatic transcriptomics with RNA-sequence analysis of antibiotic-treated and conventional mice. A total of 760 genes were differentially expressed (376 increased and 384 decreased) between antibiotic treated and conventional mice (Fig. 5A; FDR cutoff < 0.05). Ingenuity Pathway Analysis (IPA) revealed involvement in pathways related to xenobiotic metabolism and amino acid metabolism (Fig. 5B). Differences in gene expression between conventional and antibiotic-treated mice were confirmed through reverse-transcription quantitative PCR analysis of select genes related to xenobiotic and amino acid metabolism (Supporting Fig. S3).

There was a general decrease in phase-2 enzymes associated with xenobiotic metabolism such as glutathione synthesis and transferase genes (glutamate-cysteine ligase catalytic subunit [*Gclc*], glutathione S-transferase A1 [*Gsta1*], and glutathione S-transferase Mu 1 [*Gstm1*]), similar to what has been published in germ-free mice.⁽²⁴⁾ Analysis of cytochrome p450 enzyme expression demonstrated that of 49 P450 enzymes with predominant hepatic expression, four (cytochrome P450 [*Cyp*] *2c29*, *Cyp2e1*, *Cyp2u1*, and *Cyp4f15*) demonstrated differential expression with an FDR < 0.05.⁽²⁵⁾ Although there was a modest yet significant increase in xenobiotic metabolism-related phase-1 enzyme *Cyp2e1* (log₂ 0.54, FDR = 5.71×10^{-3}), there were no changes in related enzymes *Cyp1a2* and *Cyp3a11*. There was no change in upstream regulator of xenobiotic metabolism pregnane x receptor (PXR; *NR1i2*, log₂ 0.265; FDR = 0.141) but a significant increase in constitutive androstane receptor (CAR; *NR1i3*, log₂ 0.734; FDR = 0.0095).

IPA upstream pathway analysis revealed significant down-regulation in multiple chemical drug/toxin-related pathways (gentamicin, carbon tetrachloride, tunicamycin, and nitrofurantoin), reflecting changes in xenobiotic metabolism. These pathways induce significant endoplasmic reticulum (ER) stress, suggesting that microbiota depletion may attenuate the cellular response to ER stress. This is further supported by inhibition of genes associated with transcription regulator activating transcription factor 4 (ATF4) (*P* value = 1.13×10^{-7} ; activation z-score = -3.1), a key factor in the cellular integrated stress response and ER-stress response.

Nearly all of the genes associated with amino acid degradation pathways were increased (Supporting Table S2; Supporting Fig. S3). For example, genes associated with L-proline metabolism and the urea cycle (proline dehydrogenase [*Prodh*], ornithine aminotransferase [*Oat*], argininosuccinate synthase 1 [*Ass1*], and argininosuccinate lyase [*Asl*]) were increased in addition to those associated with metabolizing amino acids such as methionine into TCA cycle substrates (methionine adenosyltransferase 1A [*Mat1a*], adenosylhomocysteinase [*Ahcy*], cystathionine gamma-lyase [*Cth*], and betaine—homocysteine S-methyltransferase [*Bhmt1/2*]). Together this suggests a global shift in hepatic amino acid metabolism.

Discussion

Germ-free mice are an indispensable tool in elucidating the role of the microbiota in development, health, and disease. Nonetheless, many of the metabolic, immune, and transcriptomic signatures associated with germ-free mice are unique to the germ-free state and cannot be recapitulated by antibiotic-mediated microbiome depletion.⁽¹⁸⁾ In contrast to findings in germ-free mice, we were unable to demonstrate a meaningful relationship between microbial-derived SCFAs and global hepatic histone acetylation patterns after systematically using multiple experimental models to probe various mechanisms by which microbiota-dependent SCFAs might have an effect. These included antibiotic-mediated microbiome depletion, direct acetate feeding, and fermentable fiber feeding to modulate luminal and portal SCFA concentrations as well as a model of acute liver injury to promote hepatocyte replication. Antibiotic treatment dramatically reduced SCFA concentrations in the gut, approximating the germ-free state, yet there were only nominal effects in global hepatic histone acetylation patterns. We provide a mechanistic explanation for lack of any effect by showing that portal vein concentrations of lumenally derived butyrate are too low to inhibit hepatic HDAC enzymatic activity.

Despite having no effect on global histone acetylation patterns, we did observe that lumenally derived acetyl-CoA from direct acetate feeding was incorporated at low, yet statistically significant levels into hepatic histones, suggesting a potential role for microbially derived acetate as a substrate source for the acetylation of histones in the liver. This is consistent with recent *in vitro* data, that only during periods of cellular stress does acetate become an important source of acetyl-CoA.⁽²⁶⁾

The luminal microbiota has been shown to play a role in determining the hepatic histone acetylation landscape in microbial-naïve germ-free mice, as Krautkramer et al. demonstrated through inoculation of germ-free mice with luminal bacteria.⁽⁸⁾ However, differences in global histone acetylation landscapes between germ-free and conventional mice may be specific to the germ-free state. The inability of antibiotic-mediated microbiota depletion to recapitulate the findings observed in germ-free mice suggests that the transition from a germ-free to a colonized mouse leads to resilient alterations in hepatic histone acetylation states that cannot be altered by further modulation of the microbial environment. This finding is distinct from other germ-free phenotypes that are considered to be partially reversible, with clear alterations in their function observed after antibiotic treatment.⁽¹³⁾

Evidence for this paradigm exists in cellular development. In embryonic stem cells, exposure to differentiation signals results in an irreversible loss of a stem cell phenotype even after removal of differentiation signals. Similarly, major chromatin reorganization driven by histone acetylation leads to markers of differentiation, and addition of targeted differentiation signals induces events to stabilize these histone acetylation patterns—a key feature of embryonic development and terminal cellular differentiation.⁽²⁷⁾ Together this suggests that the differences in histone acetylation patterns seen between germ-free and conventionally raised mice may be a developmental-like effect of hepatocytes not yet exposed to microbial by-products.

Although there is an 8-log decrease in bacterial load and loss of cecal SCFAs after antibiotic treatment, there is not a comparable decrease in portal acetate and butyrate. Even without antibiotic treatment butyrate is reduced by 3-logs between the gut lumen and the portal circulation likely due to incomplete absorption of butyrate as well as intestinal epithelial metabolism of SCFAs. It is therefore possible that epithelial metabolism of butyrate may have been modified by the reduction in bacterial load so that the differential proportions in the cecum do not correlate with levels in the portal circulation. Unlike butyrate, acetate is produced by mammalian hosts likely resulting in the modest reduction of portal levels of acetate relative to the robust decrease observed in the cecum. Similarly, circulating SCFA levels are minimally different between control and antibiotic treated mice due to homeostatic effects of host hepatic and extra-hepatic metabolism.⁽²⁸⁾ Conversely even in germ free mice where there is no microbial contribution, portal levels of acetate or butyrate do not differ from antibiotic-treated mice (Supporting Fig. S4A,B).[†]

Genetic and pharmacologic inhibition of HDAC leads to changes in the dynamics of liver injury and regeneration.⁽²⁹⁾ Here we show the degree of global histone acetylation changes after acute liver injury throughout histones H3, H3.3, and H4, consistent with a role for HDAC inhibition in liver injury. Similar to our findings, H3:K9 acetylation is decreased after partial hepatectomy, although increased in ethanol-induced liver injury.⁽³⁰⁾ Nonetheless, we describe acetylation changes between injured and uninjured mice, but not between antibiotic treated and untreated mice, further demonstrating that hepatic histones acetylation is not mediated primarily by the gut microbiota.

We demonstrate gut microbiota-dependent modification in the hepatic transcriptome with prominent alterations in xenobiotic metabolism and amino acid metabolism pathways, independent of global acetylation changes. Reduction of gut bacterial load may subsequently lead to changes in the hepatic transcriptome through various mechanisms, including (1) decreased influx of bacterial products and pathogen-associated molecular patterns such as lipopolysaccharide⁽³¹⁾; (2) decreased and/or altered bacterial metabolites from metabolism of dietary constituents such as plant polyphenols and aromatic amino acids⁽³²⁾; and (3) altered bile acids and steroid hormones that can serve as ligands for nuclear receptors such as CAR and PXR, which regulate transcription of xenobiotic metabolism genes.⁽³³⁾ For example, lipopolysaccharide has been shown to decrease the expressions of cytochrome P450 enzymes,⁽³¹⁾ and bacterially dependent modification of primary into secondary bile acids, such as lithocholic acid, can increase expression of Cyp3a through activation of PXR and CAR.⁽³⁴⁾ Additionally, specific taxa in the gut microbiota are capable of metabolizing aromatic amino acids such as tryptophan into indole-3-propionic acid, a ligand for PXR.⁽³⁵⁾ Consistent with this, we observed alterations in PXR and CAR downstream target genes related to xenobiotic metabolism and an increase in CAR gene expression.

Antibiotic treatment also increased the expression of genes in pathways related to hepatic amino acid degradation, an observation that has not been described previously in germ-free mice. For example, genes related to the urea cycle and production of TCA cycle substrates were more highly expressed, suggesting that reduction of gut microbiota biomass increases hepatic amino acid bioavailability, promoting a shift in hepatic energy metabolism. Indeed, germ-free mice have been shown to have elevated portal vein levels of amino acids including

histidine, methionine and proline, amino acids whose degradation pathways we show are up-regulated after antibiotic treatment.⁽³⁶⁾ Similarly, conventional mice fed a high-protein diet demonstrate an increase in hepatic gene expression associated with amino acid catabolism.⁽³⁷⁾ These observations are consistent with the notion that the gut microbiota may compete with the host for proteins and amino acids—nitrogen sources that are critical for the growth of both eukaryotic and prokaryotic forms of life.

Alternatively, increased amino acid degradation could indicate a shift in hepatic energy metabolism from carbon to nitrogen-based energy sources. In the setting of decreased SCFA availability, the liver may undergo a programmed metabolic switch to metabolize amino acids into TCA substrates. Evidence for this shift in energy use has been demonstrated in germ-free mice that experience skeletal muscle atrophy, paired with changes in hepatic and serum amino acid levels.⁽³⁸⁾ Consequently, supplementation with SCFAs partially reverses this catabolic process and restores carbon energy use by the liver.

We further identified down-regulation of genes associated with the ATF-4 pathway, a key component of the integrated stress response (ISR), suggesting that antibiotic treatment leads to a decrease in ER stress. The ISR is a cellular cytoprotective pathway activated by cellular stress including amino acid deprivation, thereby promoting cellular adaptation of nutritional stress. Treatment of mice with microbiota-depleting antibiotics alone is sufficient to decrease expression of ER stress-related genes,⁽³⁹⁾ and the increased amino acid levels noted in germ-free mice may similarly dampen activation of ISR-associated pathways to cellular stress through ATF-4. This can potentially be seen through the significant correlation in murine studies between germ-free or antibiotic-treated mice and ATF4-deficient mice, pointing to ATF-4 as a link between the gut microbiome and hepatic response to injury.⁽⁴⁰⁾

In total, it is most likely that the observed alterations in gene expression induced by antibiotic treatment reflect microbiota-dependent metabolite and/or other small molecule alterations in the luminal environment of the gut that influence hepatic physiology through the portal circulation. Despite the inability of our antibiotic intervention to alter global histone acetylation patterns, it is still possible that significant SCFA-dependent histone acetylation alterations occur at specific gene loci. Such changes may be observed through targeted ChIP-sequencing experiments but not quantifiable by the methodologies used in our study.

In conclusion, we demonstrate that luminal SCFAs do not directly modulate histone acetylation in conventionally raised mice and that global histone acetylation changes noted in germ-free mice are likely a unique developmental phenotype that cannot be recapitulated with antibiotic-mediated microbiota depletion. Furthermore, it is important to consider the pharmacokinetics and pharmacodynamics of gut microbiota-produced metabolites that are at high levels in the gut lumen with much lower levels systemically and therefore do not translate into a biological effect. These findings underscore the significant differences between these model systems that should be taken into account when considering their relevance to human biology.

Supplementary Material

Refer to Web version on PubMed Central for supplementary material.

Acknowledgments:

The authors would like to thank Dr. John Tobias and the Next-Generation Sequencing Core for their assistance.

Supported by the H-MARC core in the Center for Molecular Studies in Digestive and Liver Disease (P30 DK 050306); Microbial Culture and Metabolomics Core in the PennCHOP Microbiome Program; Princeton-Penn Diabetes Research Center Metabolomics Core; Penn Training Program in Gastrointestinal Sciences (T32 DK 007066 to Y.S.); and American Diabetes Association Postdoctoral Fellowship (1-17-PDF-076 to C.J.).

Abbreviations:

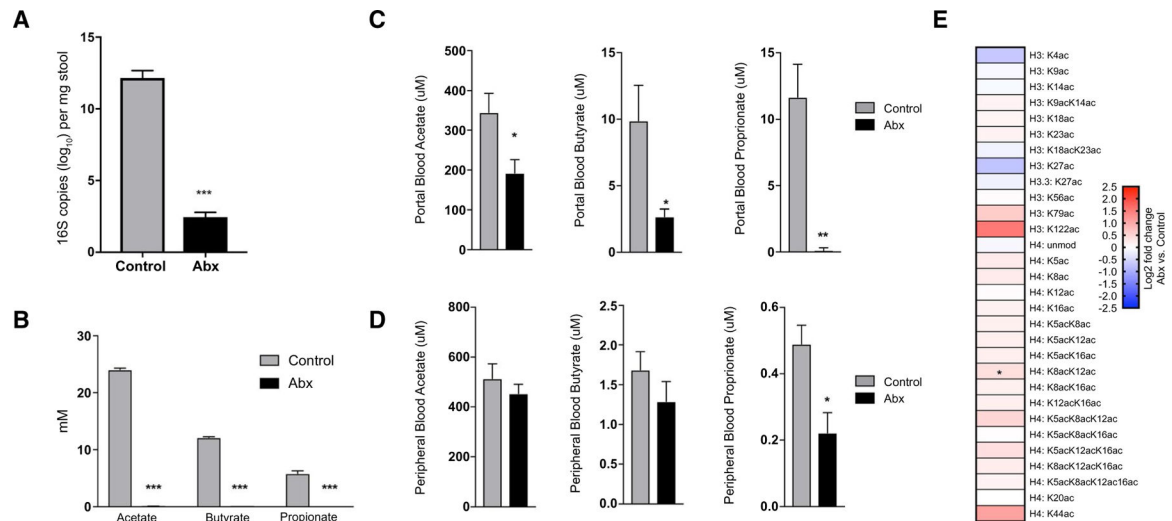
AML12	alpha mouse liver 12
CAR	constitutive androstane receptor
CCL4	carbon tetrachloride
CoA	coenzyme A
Cyp	cytochrome P450
ER	endoplasmic reticulum
FDR	false discovery rate
HAT	histone acetyltransferase
HDAC	histone deacetylase
IPA	Ingenuity Pathway Analysis
ISR	integrated stress response
PXR	pregame x receptor
SCFA	short chain fatty acid
TCA	trichloroacetic acid

REFERENCES

- 1). Tessarz P, Kouzarides T. Histone core modifications regulating nucleosome structure and dynamics. *Nat Rev Mol Cell Biol* 2014;15:703–708. [PubMed: 25315270]
- 2). Sivanand S, Viney I, Wellen KE. Spatiotemporal control of acetyl-CoA metabolism in chromatin regulation. *Trends Biochem Sci* 2018;43:61–74. [PubMed: 29174173]
- 3). Vogelauer M, Wu J, Suka N, Grunstein M. Global histone acetylation and deacetylation in yeast. *Nature* 2000;408:495–498. [PubMed: 11100734]
- 4). Imoberdorf RM, Topalidou I, Strubin M. A role for gcn5-mediated global histone acetylation in transcriptional regulation. *Mol Cell Biol* 2006;26:1610–1616. [PubMed: 16478983]
- 5). McBrien M, Behbahan I, Ferrari R, Su T, Huang T-W, Li K, et al. Histone acetylation regulates intracellular pH. *Mol Cell* 2013;49:310–321. [PubMed: 23201122]

- 6). Wu L-M, Yang Z, Zhou L, Zhang F, Xie H-Y, Feng X-W, et al. Identification of histone deacetylase 3 as a biomarker for tumor recurrence following liver transplantation in HBV-associated hepatocellular carcinoma. *PLoS One* 2010;5:e14460. [PubMed: 21206745]
- 7). Wang GL, Salisbury E, Shi X, Timchenko L, Medrano EE, Timchenko NA. HDAC1 cooperates with C/EBPalpha in the inhibition of liver proliferation in old mice. *J Biol Chem* 2008;283:26169–26178. [PubMed: 18622015]
- 8). Krautkramer KA, Kreznar JH, Romano KA, Vivas EI, Barrett-Wilt GA, Rabaglia ME, et al. Diet-microbiota interactions mediate global epigenetic programming in multiple host tissues. *Mol Cell* 2016;64:982–992. [PubMed: 27889451]
- 9). Carrer A, Parris JLD, Trefely S, Henry RA, Montgomery DC, AnnMarie Torres, et al. Impact of a high-fat diet on tissue acyl-CoA and histone acetylation levels. *J Biol Chem* 2017;292:3312–3322. [PubMed: 28077572]
- 10). Mollica MP, Mattace Raso G, Cavaliere G, Trinchese G, De Filippo C, Aceto S, et al. Butyrate regulates liver mitochondrial function, efficiency, and dynamics in insulin-resistant obese mice. *Diabetes* 2017;66:1405–1418. [PubMed: 28223285]
- 11). Mazagova M, Wang L, Anfora AT, Wissmueller M, Lesley SA, Miyamoto Y, et al. Commensal microbiota is hepatoprotective and prevents liver fibrosis in mice. *FASEB J* 2015;29:1043–1055. [PubMed: 25466902]
- 12). De Minicis S, Rychlicki C, Agostinelli L, Saccomanno S, Candelaresi C, Trozzi L, et al. Dysbiosis contributes to fibrogenesis in the course of chronic liver injury in mice. *HEPATOLOGY* 2014;59:1738–1749. [PubMed: 23959503]
- 13). Kennedy EA, King KY, Baldrige MT. Mouse microbiota models: comparing germ-free mice and antibiotics treatment as tools for modifying gut bacteria. *Front Physiol* 2018;9:1534. [PubMed: 30429801]
- 14). Shen T-C, Albenberg L, Bittinger K, Chehoud C, Chen Y-Y, Judge CA, et al. Engineering the gut microbiota to treat hyperammonemia. *J Clin Invest* 2015;125:2841–2850. [PubMed: 26098218]
- 15). Lund PJ, Kori Y, Zhao X, Sidoli S, Yuan ZF, Garcia BA. Isotopic labeling and quantitative proteomics of acetylation on histones and beyond. *Methods Mol Biol* 2019;1977:43–70. [PubMed: 30980322]
- 16). Schmittgen TD, Livak KJ. Analyzing real-time PCR data by the comparative C(T) method. *Nat Protoc* 2008;3:1101–1108. [PubMed: 18546601]
- 17). Liu X, Cooper DE, Cluntun AA, Warmoes MO, Zhao S, Reid MA, et al. Acetate production from glucose and coupling to mitochondrial metabolism in mammals. *Cell* 2018;175:502–513.e513. [PubMed: 30245009]
- 18). Zarrinpar A, Chaix A, Xu ZZ, Chang MW, Marotz CA, Saghatelian A, et al. Antibiotic-induced microbiome depletion alters metabolic homeostasis by affecting gut signaling and colonic metabolism. *Nat Commun* 2018;9:2872. [PubMed: 30030441]
- 19). Steliou K, Boosalis MS, Perrine SP, Sangerman J, Faller DV. Butyrate histone deacetylase inhibitors. *Biores Open Access* 2012;1:192–198. [PubMed: 23514803]
- 20). Waldecker M, Kautenburger T, Daumann H, Busch C, Schrenk D. Inhibition of histone-deacetylase activity by short-chain fatty acids and some polyphenol metabolites formed in the colon. *J Nutr Biochem* 2008;19:587–593. [PubMed: 18061431]
- 21). Cai L, Sutter BM, Li B, Tu BP. Acetyl-CoA induces cell growth and proliferation by promoting the acetylation of histones at growth genes. *Mol Cell* 2011;42:426–437. [PubMed: 21596309]
- 22). Murata K, Hamada M, Sugimoto K, Nakano T. A novel mechanism for drug-induced liver failure: inhibition of histone acetylation by hydralazine derivatives. *J Hepatol* 2007;46:322–329. [PubMed: 17156885]
- 23). Selwyn FP, Cheng SL, Bammler TK, Prasad B, Vrana M, Klaassen C, et al. Developmental regulation of drug-processing genes in livers of germ-free mice. *Toxicol Sci* 2015;147:84–103. [PubMed: 26032512]
- 24). Selwyn FP, Cui JY, Klaassen CD. RNA-seq quantification of hepatic drug processing genes in germ-free mice. *Drug Metab Dispos* 2015;43:1572–1580. [PubMed: 25956306]
- 25). Renaud HJ, Cui JY, Khan M, Klaassen CD. Tissue distribution and gender-divergent expression of 78 cytochrome P450 mRNAs in mice. *Toxicol Sci* 2011;124:261–277. [PubMed: 21920951]

- 26). Wellen KE, Hatzivassiliou G, Sachdeva UM, Bui TV, Cross JR, Thompson CB. ATP-citrate lyase links cellular metabolism to histone acetylation. *Science* 2009;324:1076–1080. [PubMed: 19461003]
- 27). Kim JM, Liu H, Tazaki M, Nagata M, Aoki F. Changes in histone acetylation during mouse oocyte meiosis. *J Cell Biol* 2003;162:37–46. [PubMed: 12835313]
- 28). Zhao S, Jang C, Liu J, Uehara K, Gilbert M, Izzo L, et al. Dietary fructose feeds hepatic lipogenesis via microbiota-derived acetate. *Nature* 2020;579:586–591. [PubMed: 32214246]
- 29). Xia J, Zhou Y, Ji H, Wang Y, Wu Q, Bao JJ, et al. Loss of histone deacetylases 1 and 2 in hepatocytes impairs murine liver
- 30). Huang J, Barr E, Rudnick DA. Characterization of the regulation and function of zinc-dependent histone deacetylases during rodent liver regeneration. *HEPATOLOGY* 2013;57:1742–1751. [PubMed: 23258575]
- 31). Moriya N, Kataoka H, Fujino H, Nishikawa J, Kugawa F. Effect of lipopolysaccharide on the xenobiotic-induced expression and activity of hepatic cytochrome P450 in mice. *Biol Pharm Bull* 2012;35:473–480. [PubMed: 22466549]
- 32). Zhang LS, Davies SS. Microbial metabolism of dietary components to bioactive metabolites: opportunities for new therapeutic interventions. *Genome Med* 2016;8:46. [PubMed: 27102537]
- 33). Bjorkholm B, Bok CM, Lundin A, Rafter J, Hibberd ML, Pettersson S. Intestinal microbiota regulate xenobiotic metabolism in the liver. *PLoS One* 2009;4:e6958. [PubMed: 19742318]
- 34). Toda T, Saito N, Ikarashi N, Ito K, Yamamoto M, Ishige A, et al. Intestinal flora induces the expression of Cyp3a in the mouse liver. *Xenobiotica* 2009;39:323–334. [PubMed: 19350455]
- 35). Dodd D, Spitzer MH, Van Treuren W, Merrill BD, Hryckowian AJ, Higginbottom SK, et al. A gut bacterial pathway metabolizes aromatic amino acids into nine circulating metabolites. *Nature* 2017;551:648–652. [PubMed: 29168502]
- 36). Mardinoglu A, Shoaie S, Bergentall M, Ghaffari P, Zhang C, Larsson E, et al. The gut microbiota modulates host amino acid and glutathione metabolism in mice. *Mol Syst Biol* 2015;11:834. [PubMed: 26475342]
- 37). Schwarz J, Tome D, Baars A, Hooiveld GJ, Muller M. Dietary protein affects gene expression and prevents lipid accumulation in the liver in mice. *PLoS One* 2012;7:e47303. [PubMed: 23110065]
- 38). Lahiri S, Kim H, Garcia-Perez I, Reza MM, Martin KA, Kundu P, et al. The gut microbiota influences skeletal muscle mass and function in mice. *Sci Transl Med* 2019;11:eaa5662. [PubMed: 31341063]
- 39). Fujisaka S, Ussar S, Clish C, Devkota S, Dreyfuss JM, Sakaguchi M, et al. Antibiotic effects on gut microbiota and metabolism are host dependent. *J Clin Invest* 2016;126:4430–4443. [PubMed: 27775551]
- 40). Li K, Xiao Y, Yu J, Xia T, Liu B, Guo Y, et al. Liver-specific gene inactivation of the transcription factor ATF4 alleviates alcoholic liver steatosis in mice. *J Biol Chem* 2016;291: 18536–18546. [PubMed: 27405764]

**FIG. 1.**

Antibiotic-mediated gut microbiome depletion and its effects on cecal and serum concentrations of SCFAs and hepatic histone acetylation. (A) Log₁₀ bacterial 16S copy number in control and antibiotic-treated mice. Cecal (B), portal serum (C), and peripheral serum (D) SCFA concentrations in control and antibiotic treated mice. (E) Heatmap of hepatic histone acetylation changes in antibiotic-treated mice versus control mice. Log₂ fold change is color-coded with index shown to the right of the heatmap (n = 5 mice per group). Unpaired Student *t* test; **P* < 0.05, ***P* < 0.01, ****P* < 0.001. All error bars are SEM. Abbreviation: Abx, antibiotic-treated mice.

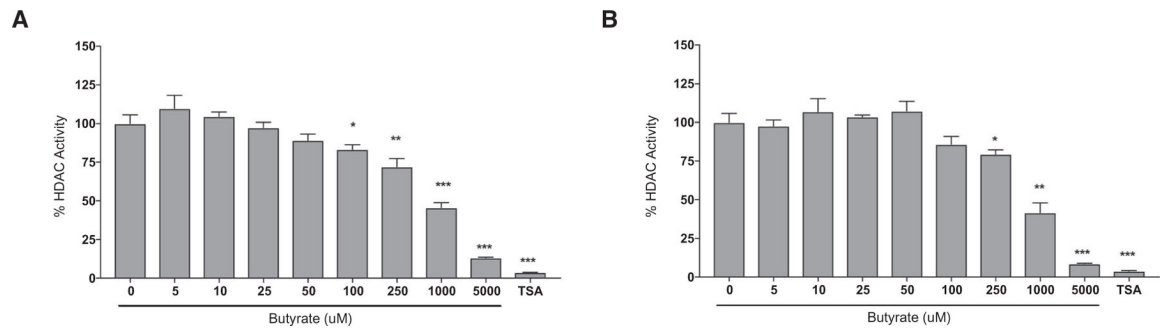
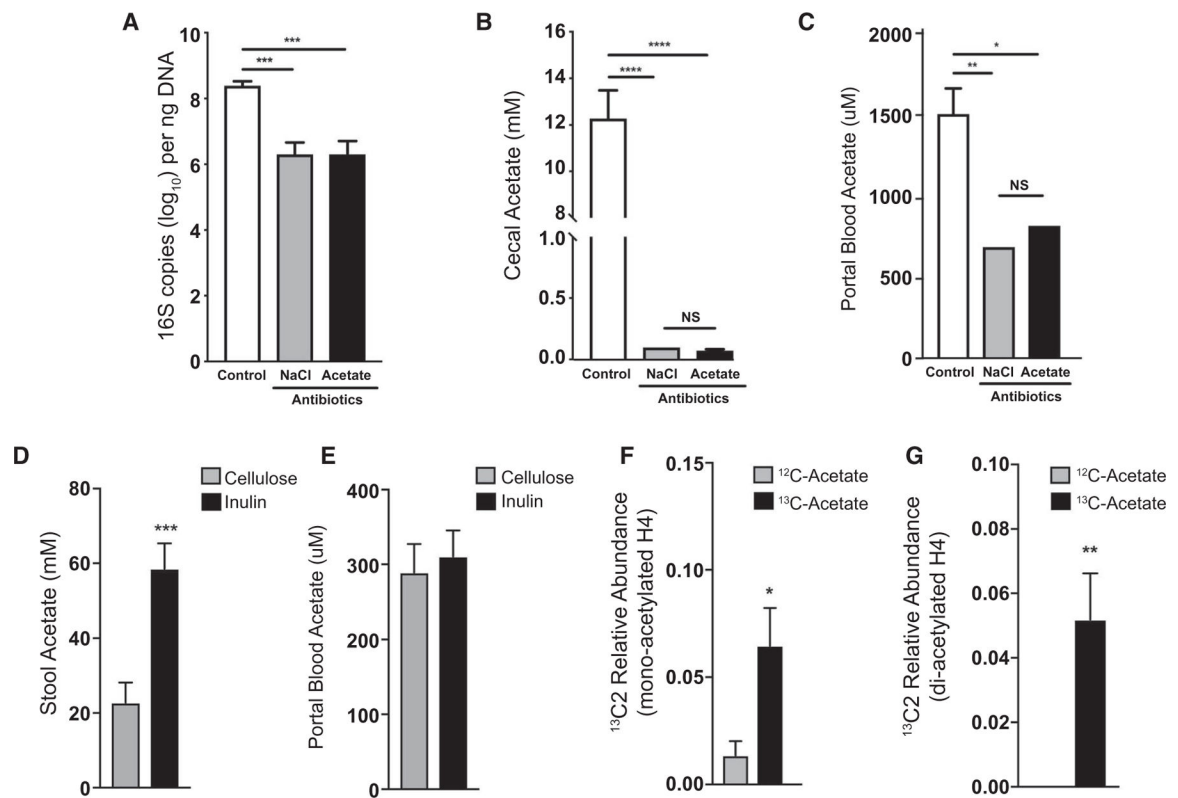
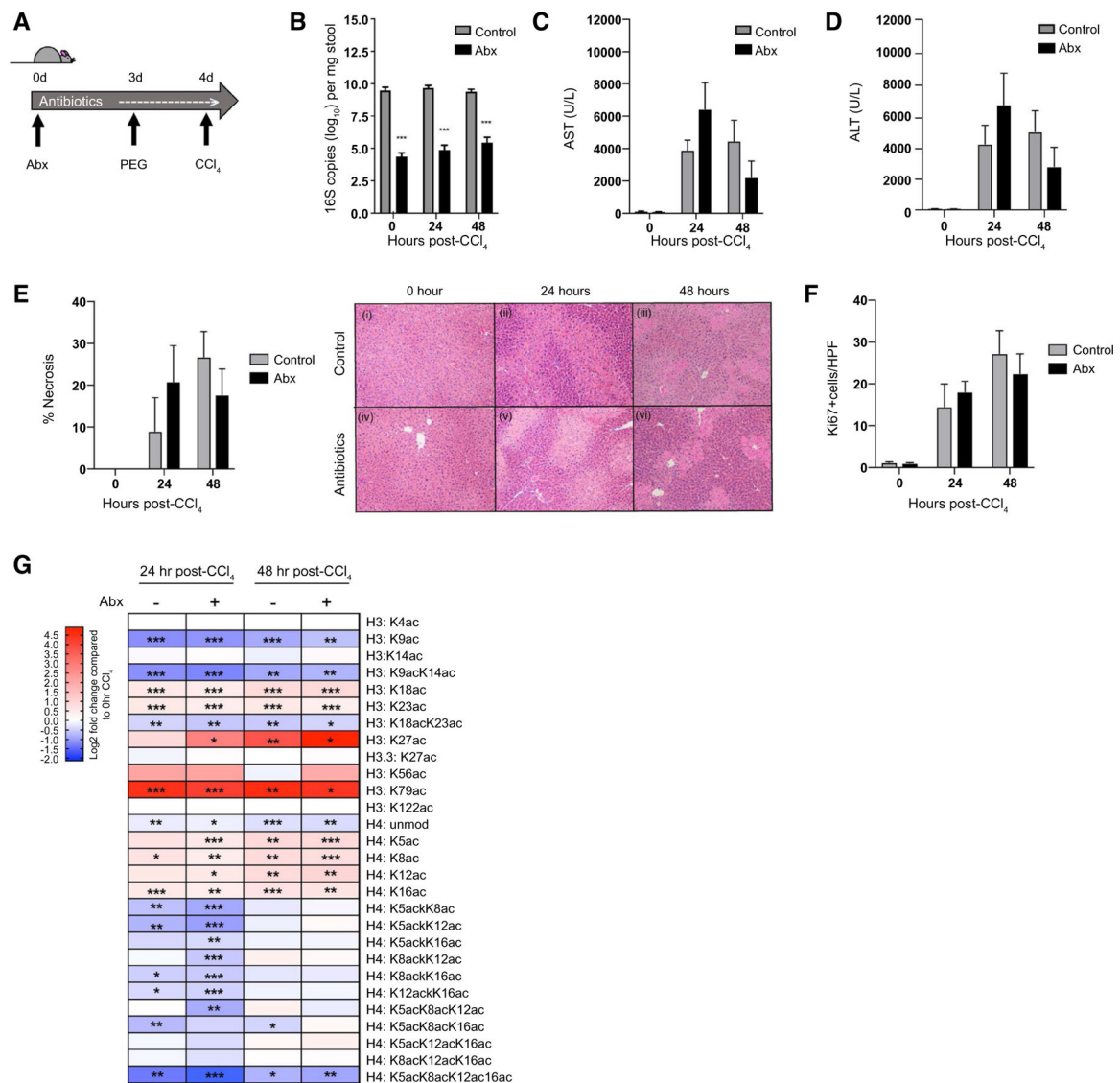


FIG. 2. Butyrate inhibition of HDAC enzymatic activity. Percent inhibition of HDAC 1 and 2 in AML12 (A) and Huh7 (B) cell lines with increasing concentrations of sodium butyrate. Trichostatin A was used as a positive control for HDAC inhibition. Experiments were performed in technical triplicates and biological doublets. Unpaired Student *t* test; * $P < 0.05$, ** $P < 0.01$, *** $P < 0.001$. All error bars are SEM. Abbreviation: TSA, trichostatin A.

**FIG. 3.**

Effect of dietary supplementation with acetate or fermentable fiber on global hepatic histone acetylation. Log₁₀ bacterial 16S copy number (A), cecal (B), and portal vein acetate concentration (C) after antibiotic treatment and supplementation with acetate in drinking water for 3 days. Cecal and portal vein acetate concentration in control mice not treated with antibiotics is shown in white. Stool (D) and portal vein acetate concentration (E) in mice fed a diet supplemented with either cellulose or inulin. Relative abundance of mono-¹³C-labeled (F) or di-¹³C-labeled (G) acetyl groups on hepatic histones in mice fed either ¹²C-acetate or ¹³C-acetate (n = 5 mice per group for [A], [B], [C], [F], and [G]; n = 8–10 for [D] and [E]). Unpaired Student *t* test; **P* < 0.05, ***P* < 0.01, ****P* < 0.001, *****P* < 0.0001. All error bars are SEM.

**FIG. 4.**

Microbiota depletion and global hepatic histone acetylation after acute CCl₄ injury. (A) Experimental diagram of acute liver injury with CCl₄ after antibiotic treatment. (B) Log₁₀ bacterial 16S copy number at 0 (baseline), 24 and 48 hours after administration of CCl₄ in control and antibiotic treated mice. Aspartate aminotransferase (C) and alanine aminotransferase (D) levels at 0 (baseline), 24 and 48 hours after administration of CCl₄ in control and antibiotic-treated mice. (E) Histological analysis of hepatic necrosis at 0, 24, and 48 hours after administration of CCl₄ in control and antibiotic-treated mice (magnification $\times 100$). (F) Quantification of Ki67-positive cells per $\times 400$ field at 0, 24, and 48 hours after administration of CCl₄ in control and antibiotic-treated mice. (G) Log₂-fold change of histone acetylation in CCl₄-treated mice compared with uninjured controls in both antibiotic-treated and untreated groups (n = 5 mice per group). Unpaired Student *t* test; **P* < 0.05 ***P* < 0.01, ****P* < 0.001. All error bars are SEM. Abbreviations: Abx, antibiotics;

ALT, alanine aminotransferase; AST, aspartate aminotransferase; CCl₄, carbon tetrachloride and PEG, polyethylene glycol.

Author Manuscript

Author Manuscript

Author Manuscript

Author Manuscript

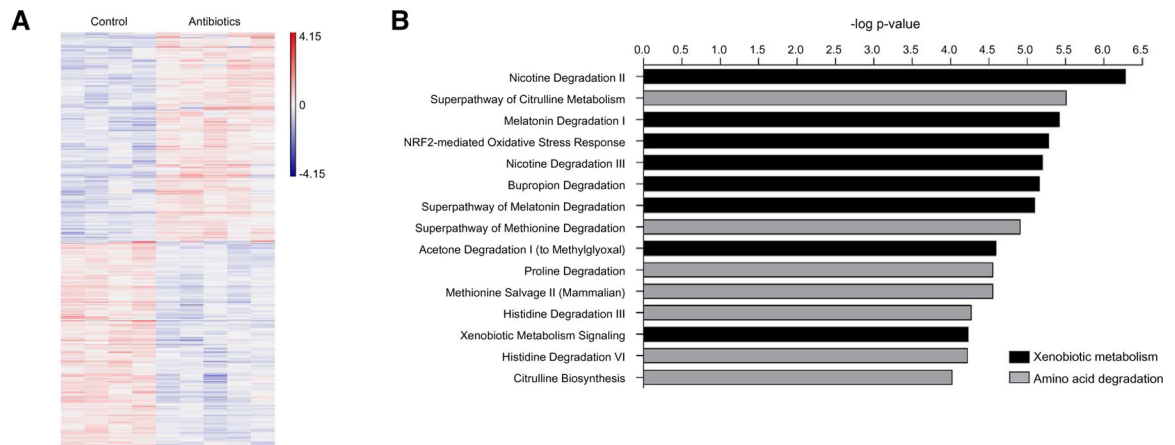


FIG. 5. Transcriptomic alterations in hepatic gene expression associated with antibiotic-mediated microbiota depletion. (A) K-means clustering of all differentially expressed genes with FDR < 0.05. (B) Functional annotation of differentially expressed genes using IPA, showing the top 15 canonical pathways (n = 4–5 mice per group). Abbreviation: NRF2, nuclear factor-erythroid 2-related factor 2.